Segmentation of Diabetic Retinopathy Based on Retinal Fundus Images Using Thresholding Technique

Nur Hasanah Ali[1](✉), Nur Asyiqin Amir Hamzah[1], Norhashimah Mohd Saad[2], Rania Mahfooz[3], and Abdul Rahim Abdullah[4]

[1] Faculty of Engineering and Technology, Multimedia University, Melaka, Malaysia
hasanah.ali@mmu.edu.my
[2] Faculty of Electrical and Electronic Engineering Technology, Universiti Teknikal Malaysia Melaka, Melaka, Malaysia
[3] Oriental Melaka Straits Medical Centre, Melaka, Malaysia
[4] Faculty of Electrical Engineering, Universiti Teknikal Malaysia Melaka, Melaka, Malaysia

Abstract. Diabetic Retinopathy is damage to the retina caused by complications of diabetes mellitus. Exudates are the primary sign of Diabetic Retinopathy identified on the opthalmoscope as white or yellowish areas with varying sizes, shapes and locations in the retina. Early detection can potentially reduce the risk of blindness. Diabetic retinopathy diagnosis for early-stage detection used a manual or semi-automated system that only an ophthalmologist can do it. This project proposed an automatic analysis of diabetic retinopathy and lesion of the eye in the retinal region using image processing techniques. The proposed technique is using thresholding technique. The data is taken from the DIRECTDB1 database. Preprocessing is applied first and then the image is segmented into 8 x 8 regions. An image histogram is then been calculated at each region to look for the maximum number of pixels for each intensity level. By comparing normal and exudate regions, the best threshold is found. The proposed technique is validated based on the accuracy, specificity, and sensitivity of exudate detection from the ground truth image reference. The mean from the range of the abnormal region of interest (ROI) is also calculated whether it is within range of the optimal value. In conclusion, adaptive thresholding is the method of choice to develop an automated detection of diabetic retinopathy. The result shows an accuracy of 65.79%, sensitivity is 31.58%, and specificity is 100%. The best segmentation and classification performance is achieved in the range of abnormal region ROI which is 0.35 to 0.55.

Keywords: Diabetic retinopathy · segmentation · thresholding · retina fundus image

1 Introduction

The defects in insulin secretion, insulin action or both causing hyperglycemia are the characteristic of the metabolic disease diabetes [1]. Diabetes with chronic hyperglycemia

M. Y. bin Alias (Ed.): MECON 2022, AER 214, pp. 164–173, 2023.
https://doi.org/10.2991/978-94-6463-082-4_17

is associated with long-term damage, failure and dysfunction of different organs likely the eyes, kidneys, nerves, heart and blood vessels [2]. The majority of cases of diabetes fall into two categories of etiopathogenetic which are type I and type II [3]. The insulin secretion absolute deficiency is the leading cause of category type 1 diabetes. Diabetes type 2 is one of the most terrible chronic diseases caused by defects in pancreatic insulin secretion [4].

Approximately 537 million people have diabetes in the year 2021, and this case is expected to reach 643 million by 2030, and 783 million by 2045 [5]. Long-term suffering from diabetes can cause blood in veins to break onto the retina prompting vision loss and even visual deficiency. Diabetic related eye illness such as diabetic retinopathy and diabetic moculopathy has been known visual misfortune [6]. Diabetic retinopathy is a continual disease in the retina which leads to permanent vision loss or blindness. Diabetic retinopathy will lead to 1% of blindness in the world and can be prevented and curable by early detection [7].

Due to retinal abnormalities are widespread and their implications being substantial, fundus imaging plays a significant role in diabetes monitoring [8]. Fundus imaging, on the other hand, is a potential for non-invasive screening since the eye fundus is sensitive to vascular disorders. The success of this sort of screening relies on precise fundus picture collection, as well as the accuracy and reliability of the image processing methods for detecting abnormalities [9]. Many research groups have presented various algorithms for fundus image analysis. However, because there is no widely approved and representative fundus image database or evaluation process, it is not possible to assess the reliability and accuracy of the methodologies.

In local adaptive technique, a threshold is calculated for each pixel, based on some local statistics such as range, variance, or surface-fitting parameters of the neighbourhood pixels. It can be approached in different ways such as background subtraction [10] water flow model [11], mean and standard deviation of pixel values [12], and local image contrast [13]. Some draw backs of the local thresholding techniques are region size dependent, individual image characteristics, and time consuming. Therefore, some researchers use a hybrid approach that applies both global and local thresholding method [14] and some use morphological operators [15].

2 Methods

Figure 1 shows the project flow for the whole analysis. The methodology mainly divided into five parts which are image data, pre-processing image, segmentation process, and feature extraction and performance verification.

2.1 Database

The fundus images are collected publicly on the DIRECTDB1 website database consisting of 89 color fundus images of which 84 images are in the category of at least mild non-proliferative signs of diabetic retinopathy with various characteristics [16]. The image resolution is 1500 × 1520 pixels and in a PNG file. Figure 2 shows normal fundus images and does not contain any signs of diabetic retinopathy based on all experts

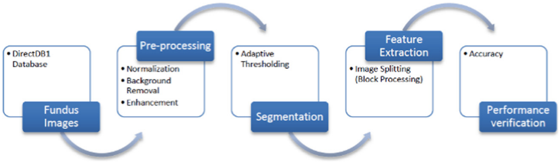

Fig. 1.

(a)

(b)

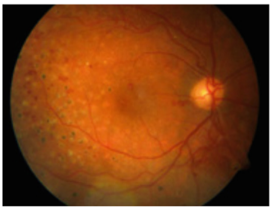

(c)

Fig. 2. Examples of DIRECTDB1 fundus images [16]: (a) normal fundus, (b) abnormal fundus, and (c) abnormal fundus after treatment by photocoagulation.

who participated in the evaluation. From the DIRECTDB1 website, the fundus images were taken in the Kuopio University Hospital. It has clarified that the picture quality of all the images is enough for medical research, the image of the patient is not replicated and a feasible commixture of ethnicity and disease stratification is repressed.

2.2 Pre-processing Stage

Figure 3 shows one of the image samples with mild proliferative diabetic retinopathy at the pre-processing stage from the RGB image (original image from the fundus camera. The R represents red with an 8-bit unsigned integer, G represents green with an 8-bit

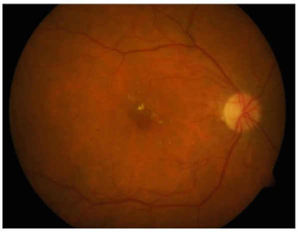

Fig. 3. The original image with green channel from fundus images

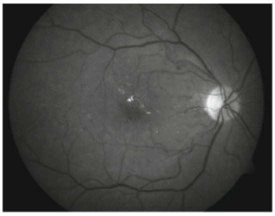

Fig. 4. The images convert to gray level with 8 bits unsigned integers (0–255).

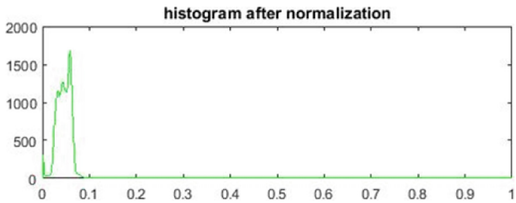

Fig. 5. The histogram based on the gray level image with an integer between 0–255.

unsigned integer and B represents blue with an 8-bit unsigned integer [1]. The green plane image generally acquires more information whereas the red acquires more brightness and has poor contrast and the blue plane image shows a darker area [1]. The fundus images are then been converted to the gray level values from 8-bit unsigned integer (0–255) as shown in Fig. 4. The '0' in pixels value with an 8-bit unsigned integer represents the black color and the '255' represents the white color.

Then the image normalized to floating point value (0 to 1) as shown in Fig. 5 with the histogram floating point value of 0 to 1. The gray level image with 8-bit unsigned integer (0–255) was applied contrast normalization so that the image with 256 pixels intensity value changes the range of pixel to floating point value 0 to 1. The background needs to be removed since it has the largest number of low pixels.

2.3 Segmentation Stage

In the segmentation stage, adaptive thresholding segmentation was applied in segmenting the exudate of the retina. The image is first divided into 8×8 macro-block regions, where 256×256 pixels are separated to 16×16 pixels in size in each region as shown in

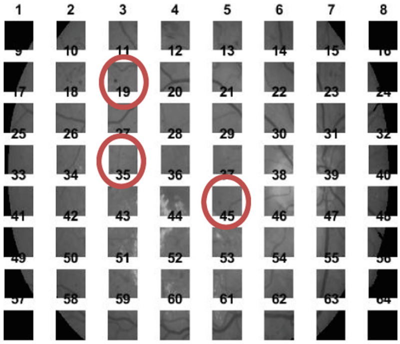

Fig. 6. 16 × 16 pixels per micro-block region

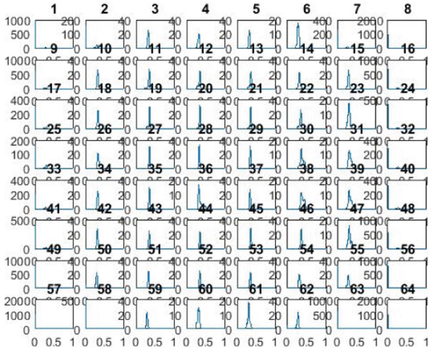

Fig. 7. The histogram distribution of each region

Fig. 6. The exudate area is indicated by the red circle in regions 19, 35 and 45. Figure 7 shows the histogram that has been calculated for each region.

The maximum number of pixels at each intensity level will be obtained from the histogram plot as shown in Fig. 8 and can be calculated using Eq. (1).

$$P_{max}(i) = Max(P(R_i : R_m, i)) \tag{1}$$

where P(i) is the intensity at level I, and R_1 to R_m are the number of pixels in i^{4th} macro-block region.

The range of abnormal region of interest (ROI) is calculated based on Eq. (2).

$$I(x, y)_{hyperintense} = \begin{cases} 1\ for\ I(x.y) \geq T \\ 0\ elsewhere \end{cases} \tag{2}$$

Figure 9 shows the overlap graph of the abnormal region and normal region. The green graph is a normal region and red graph is an abnormal region. From this graph, the mean range from the ROI histogram is between 0.35 to 0.55.

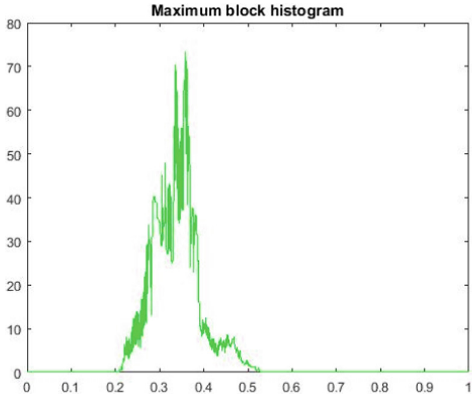

Fig. 8. The maximum block histogram.

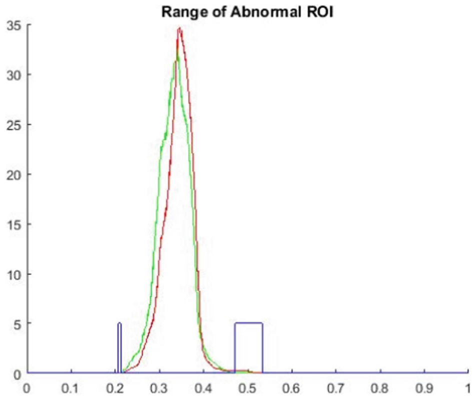

Fig. 9. The range of abnormal ROI.

2.4 Performance Assessment Matrices

The most important evaluation measures for medical diagnosis methods are sensitivity, specificity and accuracy. As suggested in Eq. (2), sensitivity is the proportion of the true positive that is correctly identified by the diagnosis test which in this project is the exudate ground truth. It demonstrates how accurate the test is at detecting disease. The fraction of true negatives found by diagnosis is referred to as specificity in this project segmentation. Its purpose is to demonstrate how accurate the test is in detecting normal (negative) conditions. The proportion of true outcomes in a population, whether true positive or true negative, is known as accuracy. It assesses the accuracy of a diagnostic test on a given condition [17]. The higher the percentage of sensitivity, it less likely the diagnostic test returns to false-positive result. The percentage of specificity refers to the probability of test diagnosing a lesion in the retina without giving false-positive results. The percentage of accuracy represents the proportion of true positive results which are true positive and true negative in the selected population [2].

The segmentation results obtained from the proposed method are compared with the ground truth reference based on the DIRECTDB1 database, drawn by an ophthalmologist. In this analysis, the result of classification was compared with the ground truth whether it has the exudate or not. Accuracy, sensitivity and specificity of the correct classification are evaluated using Eqs. (3), (4) and (5).

$$Sensitivity(SN) = \frac{T_P}{T_P + F_N} \tag{3}$$

$$Specificity(SP) = \frac{T_N}{T_N + F_P} \tag{4}$$

$$Accuracy(AC) = \frac{T_N + T_P}{T_N + T_P + F_N + F_P} \tag{5}$$

where;

T_P is the number of abnormal fundus images found as abnormal.
T_N is the number of normal fundus images.
F_P is the number of normal fundus images found as abnormal (false positive).
F_N is the number of abnormal fundus images found as normal (false negatives).

3 Results

Two evaluation principles were selected which are 1) the evaluation of mean optimal thresholding and 2) the accuracy, specificity and sensitivity. The first principle is justified by the mean of the abnormal region in the region of interest (ROI) within the optimal value of thresholding. The second principle is due to the practical fact that most researchers concentrate only on one or several finding types. The samples of 89 fundus images from the DIRECTDB1 database were collected. The images are pre-processed first to produce clearer images than the original images. The pre-processed fundus image is then segmented using the adaptive thresholding technique.

For the mean optimal thresholding method, the mean result of the optimal thresholding technique for all images based on the histogram varies in the range of 0.35 to 0.55 (Fig. 10).

As for the second method, Table 1 shows confusion matric that helps to obtain accuracy, sensitivity and specificity. T_P, F_N, F_P and T_N are calculated based on the 38 normal images and 51 abnormal images.

From the result obtained, performance verification has been achieved, where the accuracy obtained is 65.79%, sensitivity is 31.58%, and specificity is 100%. The overall performance can be improved using the recent segmentation techniques such as Fuzzy c-means, region growing, k-means, watershed, etc. [18].

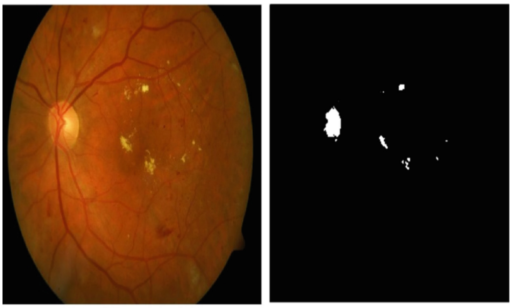

(a) (b)

Fig. 10. Example of the exudate detection from the proposed segmentation: a) The original image b) The image segmentation for Image15

Table 1. The Confusion Matrix

Description	Ground truth Exudate from the Database	
Segmentation of retina	$T_P = 0.3158$	$F_P = 0$
	$F_N = 0.6842$	$T_N = 1$

4 Conclusions

As a conclusion, diabetic retinopathy is retinopathy (damage to the retina) caused by complications of diabetes mellitus. It can eventually lead to blindness. It is an ocular manifestation of systemic disease that affects up to 80% of all patients who have had diabetes for 10 years or more. There are several stages of diabetic retinopathy. The development of many medical screening methods has led to more development in segmentation methods for automatic detections. As the manual lesion segmentation method is time consume and focus only on expert in ophthalmology. Therefore, this project is an automated segmentation classification of diabetic retinopathy characteristics based on retina fundus images.

Adaptive thresholding is the method of choice to develop an automated in detecting diabetic retinopathy. The performance of the segmentation technique is evaluated and discussed based on the accuracy is 65.79%, sensitivity is 31.58%, and specificity is 100%. The best segmentation and classification performance is achieved in the range of abnormal region ROI which is 0.35 to 0.55. The image segmentation can be improved to adapt to different intensities and contrast.

Acknowledgments. The authors would like to acknowledge funding support from Multimedia University, Malaysia.

Authors' Contributions. The main contribution of this work is to propose automated segmentation for diabetic retinopathy using fundus images. The result based on the accuracy, sensitivity and specificity were compared with the research on DIRECTDB1 work.

References

1. U. Galicia-Garcia *et al.*, "Pathophysiology of type 2 diabetes mellitus," *Int. J. Mol. Sci.*, vol. 21, no. 17, pp. 1–34, 2020, doi: https://doi.org/10.3390/ijms21176275.
2. S. I. Taylor, Z. S. Yazdi, and A. L. Beitelshees, "Pharmacological treatment of hyperglycemia in type 2 diabetes," *J. Clin. Invest.*, vol. 131, no. 2, pp. 1–14, 2021, doi: https://doi.org/10.1172/JCI142243.
3. S. Tsalamandris *et al.*, "The role of inflammation in diabetes: Current concepts and future perspectives," *Eur. Cardiol. Rev.* , vol. 14, no. 1, pp. 50–59, 2019, doi: https://doi.org/10.15420/ecr.2018.33.1.
4. L. S. Francesca Pivari, Alessandra Mingione, Caterina Brasacchio, "Curcumin and Type 2 Diabetes Mellitus: Prevention and Treatment," *Nutrients*, vol. 31, no. August, pp. 10–25, 2019.
5. Professor Rhys Williams, *International Diabetes Federation*, vol. 102, no. 2. 2021. doi: https://doi.org/10.1016/j.diabres.2013.10.013.
6. Y. Wang *et al.*, "Prevalence of and risk factors for diabetic retinopathy and diabetic macular edema in patients with early and late onset diabetes mellitus," *Ophthalmic Res.*, 2020, doi: https://doi.org/10.1159/000508335.
7. Y. Hou, Y. Cai, Z. Jia, and S. Shi, "Risk factors and prevalence of diabetic retinopathy: A protocol for meta-analysis," *Medicine (Baltimore).*, vol. 99, no. 42, p. e22695, 2020, doi: https://doi.org/10.1097/MD.0000000000022695.
8. K. Zhang, "An AI system for the detection and incidence prediction of chronic kidney disease and type 2 diabetes based on retinal fundus images," *Pap. Knowl. . Towar. a Media Hist. Doc.*, 2021.
9. S. Sudha and A. Srinivasan, "Unravelling diabetic retinopathy through image processing, neural networks, and fuzzy logic: A review," *Asian J. Pharm. Clin. Res.*, vol. 10, no. 4, pp. 32–37, 2017, doi: https://doi.org/10.22159/ajpcr.2017.v10i4.17023.
10. S. Lu, B. Su, and C. L. Tan, "Document image binarization using background estimation and stroke edges," *Int. J. Doc. Anal. Recognit.*, vol. 13, no. 4, pp. 303–314, 2010, doi: https://doi.org/10.1007/s10032-010-0130-8.
11. H. H. Oh, K. T. Lim, and S. Il Chien, "An improved binarization algorithm based on a water flow model for document image with inhomogeneous backgrounds," *Pattern Recognit.*, vol. 38, no. 12, pp. 2612–2625, 2005, doi: https://doi.org/10.1016/j.patcog.2004.11.025.
12. J. Sauvola and M. Pietikäinen, "Adaptive document image binarization," *Pattern Recognit.*, vol. 33, no. 2, pp. 225–236, 2000, doi: https://doi.org/10.1016/S0031-3203(99)00055-2.
13. B. Su, S. Lu, and C. L. Tan, "Binarization of historical document images using the local maximum and minimum," *ACM Int. Conf. Proceeding Ser.*, no. June, pp. 159–165, 2010, doi: https://doi.org/10.1145/1815330.1815351.
14. B. Gatos, I. Pratikakis, and S. J. Perantonis, "Adaptive degraded document image binarization," *Pattern Recognit.*, vol. 39, no. 3, pp. 317–327, 2006, doi: https://doi.org/10.1016/j.patcog.2005.09.010.
15. T. H. N. Le, T. D. Bui, and C. Y. Suen, "Ternary entropy-based binarization of degraded document images using morphological operators," *Proc. Int. Conf. Doc. Anal. Recognition, ICDAR*, pp. 114–118, 2011, doi: https://doi.org/10.1109/ICDAR.2011.32.
16. T. Kauppi *et al.*, "The DIARETDB1 diabetic retinopathy database and evaluation protocol," *BMVC 2007 - Proc. Br. Mach. Vis. Conf. 2007*, pp. 1–18, 2007, doi: https://doi.org/10.5244/C.21.15.

17. A. Tharwat, "Classification assessment methods," *Appl. Comput. Informatics*, vol. 17, no. 1, pp. 168–192, 2018, doi: https://doi.org/10.1016/j.aci.2018.08.003.
18. N. Hasanah Ali, A. Rahim Abdullah, N. Mohd Saad, A. Sobri Muda, T. Sutikno, and M. Hatta Jopri, "Brain stroke computed tomography images analysis using image processing: A Review," *IAES Int. J. Artif. Intell.*, vol. 10, no. 4, p. 1048, 2021, doi: https://doi.org/10.11591/ijai.v10.i4.pp1048-1059.